ELSEVIER

Journal of Molecular Catalysis A: Chemical 187 (2002) 119–128

JOURNAL OF MOLECULAR CATALYSIS A: CHEMICAL

www.elsevier.com/locate/molcata

Study of the surface acidity of an hematite powder

Luca Ferretto, Antonella Glisenti*

Dipartimento di Chimica Inorganica, Metallorganica ed Analitica, Università di Padova, Via Loredan 4, 35131 Padova, Italy

Received 10 October 2001; received in revised form 2 January 2002; accepted 14 March 2002

Abstract

In this work, the interaction between α-Fe_2O_3 (hematite) powder samples and pyridine, 2,6-dimethyl pyridine, carbon monoxide and carbon dioxide was studied, at atmospheric pressure as well as under high vacuum (HV) conditions. The powder was characterised by means of diffuse reflectance infrared Fourier transform (DRIFT) and X-ray photoelectron spectroscopies (XPS), X-ray diffraction (XRD) and thermal analysis (TGA-DSC).

Chemisorption experiments at atmospheric pressure were studied by means of DRIFT spectroscopy while those carried out under HV conditions were followed by means of quadrupolar mass spectrometry (QMS) and XPS.

The study of the interaction of pyridine with α-Fe_2O_3 allowed us to appreciate the presence of both Brönsted and Lewis acid sites on the powder surfaces. Moreover, the use of CO as probe molecule indicated the existence of non equivalent Lewis acid sites. Finally, CO_2 may interact with the powder sample either reacting with surface OH groups giving rise to bicarbonate species, or with surface cations and neighbouring oxide ions to originate bidentate carbonate species.

Keywords: Hematite; Chemisorption; Surface-acidity; Fe_2O_3; Catalysis

1. Introduction

Iron and iron oxide based catalysts have been widely used in several industrial processes such as dehydrogenation, oxidation and Fisher–Tropsch synthesis [1,2]. Nevertheless, only a few studies about the chemisorption of small inorganic and organic molecules on iron oxides have been so far published [3–20] and many aspects of the reactivity of hematite surfaces are not yet completely understood.

As a matter of fact, a detailed knowledge of the distribution and strength of the active sites of iron oxide surfaces is fundamental to understand the reactivity of iron oxide based catalyst as well as to design more active catalytic systems.

In this regard, it should be stressed that methanol chemisorbs mainly dissociatively on hematite (the formation of formate is evident at temperatures higher than 400 K [18]) while on a Fe–Ti–O mixed oxide the chemisorption is mainly molecular. Incidentally, it is also noteworthy that oxidising power of the mixed oxide is lower than that of Fe_2O_3; [21] thus the study of the acid/base and redox character of surfaces is of great relevance to look into the adsorbate–substrate interaction, as well as to get further insights into the reaction involving surface chemisorbed species.

This paper is part of an ongoing experimental and theoretical study of surface properties of iron based mixed oxides. The final goal of the present contribution is the study of the distribution of the acid/base active sites on hematite powder samples. For this

* Corresponding author. Tel.: +39-49-8275196; fax: +39-49-8275161.
E-mail address: glisenti@chin.unipd.it (A. Glisenti).

1381-1169/02/$ – see front matter
PII: S1381-1169(02)00126-7

reason the interaction of the α-Fe_2O_3 (hematite) powder with pyridine, 2,6-dimethyl pyridine (lutidine), carbon oxide and carbon dioxide was investigated.

Chemisorptions were carried out both at atmospheric pressure (in inert atmosphere) and under high vacuum (HV) conditions. In the former case the reaction was investigated by means of a FTIR spectroscopy while XPS and quadrupolar mass spectrometry (QMS) have been joined for experiments carried out in HV conditions.

It is well known [2,22] that pyridine can interact with Lewis and Brönsted acid sites (hereafter L_S^a and B_S^a, respectively) distributed on the oxide surface giving rise to different adsorbed species. Their characterisation allows to distinguish among different acid sites. At variance to that, [23–26] lutidine mainly interacts atop with exposed B_S^a as a consequence of its steric hindrance. CO is a very weak base largely used to probe L_S^a acidity while carbon dioxide is preferred for the investigation of the Lewis base sites (L_S^b) [22].

2. Experimental

2.1. Sample preparation

α-Fe_2O_3 was prepared by precipitation from an acid solution of Fe^{3+} ions. This solution was obtained dissolving 10 g of iron powder in acid solution; iron hydroxide was precipitated adding NH_4OH (Sigma–Aldrich, 28%). The precipitated was filtered and washed with bi-distilled water until pH = 7; it was then dried at 523 K in air for 12 h and calcined at 773 K in air for 6 h. Before the chemisorption in HV, the sample was processed as a pellet (the powder was pressed at 2×10^8 Pa for 10 min) and evacuated for 20 min at room temperature (RT).

2.2. Reaction conditions

Pyridine and lutidine employed for chemisorption experiments (Sigma–Aldrich, spectroscopic grade) were used without further purification.

The exposure of the pellet to pyridine and lutidine under HV conditions, was carried out at temperatures ranging from RT to 723 K, at a total pressure of ca. 4×10^{-4} Pa. Pyridine and lutidine vapours were obtained by evaporation under vacuum. The employed HV reactor, directly connected to the XPS analysis chamber, allows us to work in flow conditions; moreover, volatile products were characterized by means of a quadrupole gas analyser (European Spectrometry Systems (ESS)). Background gases contribution to the spectrum were eliminated by subtracting to the spectrum recorded after the chemisorption the one obtained just before. Mass spectra assignments have been done by referring to the fragmentation patterns [27]. Moreover, all mass data were analysed by using the method proposed by Ko et al. [28], and the temperature of the pellet was evaluated through a thermocouple directly in contact with the sample-holder.

The exposure of powder samples to probe molecules in the FTIR equipment has been done by using the Spectra-Tech. Inc. COLLECTOR™ apparatus for diffuse reflectance infrared Fourier transform (DRIFT) spectroscopy fitted with the HTHP (high temperature high pressure) chamber. In this regard it should be stressed that for the chemisorption of pyridine and lutidine, the HTHP chamber was filled with nitrogen vapours flowing through a bubbler containing the liquid while for CO and CO_2 the outlet was directly connected to the reaction chamber.

2.3. FTIR measurements

The IR spectra were obtained by means of a Bruker IFS 66 spectrometer working in diffuse reflectance mode and displayed in Kubelka–Munk units [29,30]. The resolution of the spectra was 4 cm^{-1}. The sample temperature was measured through of a thermocouple inserted into the sample holder directly in contact with the powder.

2.4. XPS measurements

XP spectra were recorded by means of a Perkin-Elmer PHI 5600 ci spectrometer with a standard Al Kα source (1486.6 eV) working at 350 W. The working pressure was less than 1×10^{-8} Pa. The spectrometer was calibrated by assuming the binding energy (BE) of the $Au_{4f7/2}$ line to be 84.0 eV with respect to the Fermi level. Extended spectra (survey) were collected in the range 0–1350 eV (187.85 eV pass energy, 0.4 eV step, 0.05 s per step). Detailed spectra were recorded for the following regions: C 1s, O 1s, Fe 2p (11.75 eV pass energy, 0.1 eV step, 0.1 s per step).

The standard deviation in the BE values of the XPS line is 0.10 eV. The atomic percentage, after a Shirley type background subtraction, [31] was evaluated using the PHI sensitivity factors [32]. To take into account charging problems the C 1s peak was considered at 285.0 eV and the peaks BE differences were evaluated.

2.5. Thermal analysis and XRD

Thermogravimetric analysis (TGA) and differential scanning calorimetry (DSC) were carried out in a controlled atmosphere using the simultaneous differential techniques (SDT) 2960 of TA Instruments. Thermograms were recorded at 4 and 10 °C min^{-1} heating rates in air or nitrogen flow. The covered temperature ranges from RT to 1273 K.

X-ray diffraction (XRD) patterns were obtained with a Philips diffractometer with Bragg-Brentano geometry using a Cu Kα radiation (40 kV, 40 mA, $\lambda = 0.154$ nm).

3. Results and discussion

3.1. Sample characterisation

The sample was characterised by means of XRD, XP and DRIFT spectroscopies as well as by thermal analysis (TGA-DSC).

XRD pattern (Table 1) coincides with that of hematite, [33] and the crystallite mean diameter is around 21 nm [34].

The XPS survey of the calcined sample shows the presence of carbon contamination while nitrogen, (another possible contaminant because of the preparation procedure) was never observed.

The $Fe_{2p_{3/2}}$ peak lies at 711.0 eV (Table 2 and Fig. 1), i.e. in comparable agreement with literature data for Fe(III) in Fe_2O_3 [35–37]. Furthermore, both the energy position of the O 1s peak position (530.0 eV) and the BE difference between O 1s and Fe $2p_{3/2}$ peaks, $\Delta BE_{(O\,1s-Fe\,2p_{3/2})}$, agree with the

Table 1
XRD data (*d*, nm) obtained for the Fe_2O_3 powder compared to the JCPDS card values

Fe_2O_3 (this work)	Fe_2O_3 (hematite)[a]
2.700 (100)	2.700 (100)
2.519 (70)	2.519 (95)
1.694 (45)	1.694 (50)
1.841 (40)	1.840 (45)
3.684 (30)	3.684 (28)
1.486 (30)	1.485 (37)
1.454 (30)	1.451 (37)
2.207 (20)	2.205 (30)

[a] Joint Committe on Powder Diffraction Standard: card number 33-664.

Table 2
XPS data (BE in eV) for Fe, Fe_2O_3 and related compounds. (The BE difference between Fe $2p_{3/2}$ and O 1s, $\Delta BE_{Fe\,2p-O\,1s}$, are also shown[a,b,c])

	Fe $2p_{3/2}$	O 1s	$\Delta BE_{Fe\,2p3/2-O\,1s}$
This work	711.0	530.0 531.0 532.7	181
α-Fe_2O_3	710.7–710.9	529.6–529.9	180.8–181.3
FeO	709.3–709.9	530.0	179.6–179.9
Fe	706.8–707.4		

[a] NIST Standard Reference Database 20, version 3.0.
[b] [32].
[c] [36].

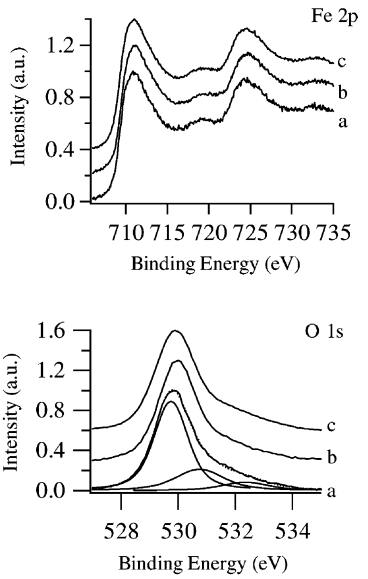

Fig. 1. Fe 2p and O_{1s} XPS spectra obtained for the α-Fe_2O_3 (hematite) powder (a) before the chemisorptions, after the chemisorption of (b) pyridine and (c) carbon dioxide at RT. The fitting results obtained processing the O_{1s} XP peak are also shown.

expected values (Fig. 1 and Table 2). The obtained O/Fe atomic ratio is 1.4. Finally, the asymmetry of the O 1s peak on its higher BE side (Fig. 1) suggests the presence of surface hydroxyl groups [35].

In principle these OH groups can be classified according to three different types: free or isolated OH groups, H bonded OH groups and OH groups interacting with chemisorbed water molecules [38,39]. The distribution of these groups is a function of the preparation conditions, such as temperature and sample dehydration degree.

The O 1s XPS peak fitting procedure shows (Fig. 1) three contributions centred around 530.0, 531.0 and 532.7 eV. The peak at 530.0 eV is due to the Fe–O bonds while the other two bands suggest the presence, on the α-Fe_2O_3 surface, of chemically non-equivalent OH groups.

The IR spectrum (at RT) of the α-Fe_2O_3 in the O–H stretching region is reported in Fig. 2a. Here a broad and intense band at ca. 3400 cm^{-1} (with a shoulder around 3200 cm^{-1}) and several quite narrow peaks at 3622, 3663, 3690 and 3740 cm^{-1} are evident.

The broad band at ca. 3400 cm^{-1} is ascribed to H-bonded water [40]. According to this assignment its intensity significantly decreases with increasing temperature (Fig. 2a). As far as the band shape is concerned it agrees with the presence of two contributions, thus suggesting the existence of water molecules interacting with the Fe_2O_3 surface in different ways. Consistently, the bending vibration peak of water (Fig. 2b) is composed by two contributions at ca. 1540 and 1640 cm^{-1}. All the remaining peaks are attributed to the stretching vibration of free (3690 and 3740 cm^{-1}) and H-bonded (3663 and 3622 cm^{-1}) OH groups. In particular, the peak at 3622 cm^{-1} correspond to OH groups H-bonded to water molecules [19].

The distribution and reactivity of these OH groups strongly depends on the preparation procedure, the sample history and the exposed faces, [41][1] thus suggesting the possibility of tuning the acid/base character of a reactive surface through an appropriate preparation route.

[1] As a matter of fact, slightly different results have been observed on an hematite sample obtained by precipitation of the hydroxide from an iron nitrate solution: the surface resulted more significantly hydrated and the peaks due to the stretching vibration of the isolated hydroxyl groups became visible only at temperatures higher then RT. See also [18,19].

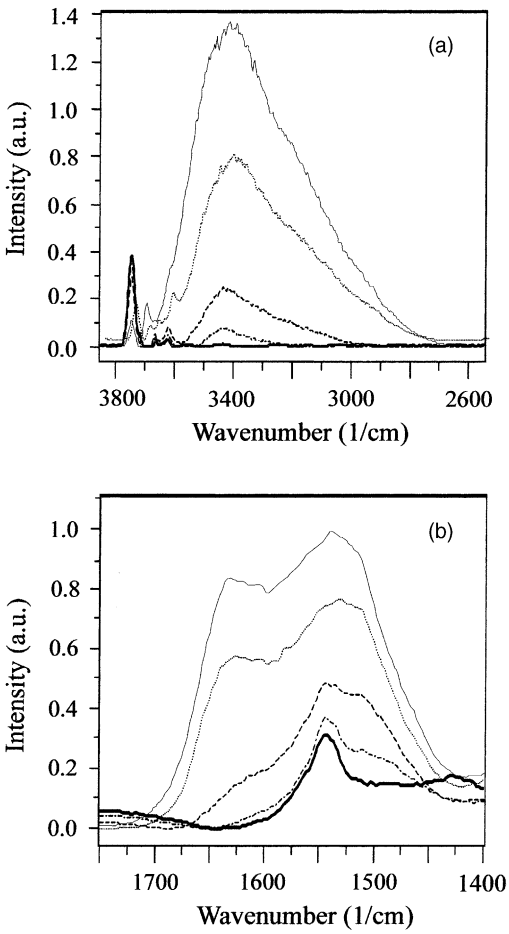

Fig. 2. IR spectra obtained for the α-Fe_2O_3 (hematite) powder before the heating treatment (—) and after the heating treatment at 323 K (···), 373 K (- - -), 423 K (–·–·–), 473 K (▬▬); (a) region between 2600 and 3800 cm^{-1}, (b) 1400 and 1750 cm^{-1}.

Moving to the analysis of TGA data the inspection of the spectrum shows that weakly bonded water is removed between 400 and 410 K; no weight loss is observed at higher temperatures. The DSC spectrum confirms the sample stability in the investigated temperature range.

3.2. Reaction with pyridine

The IR spectrum of α-Fe_2O_3 exposed at RT to a pyridine + N_2 mixture (Fig. 3) is characterised by the presence of several peaks lying at: 1639, 1606, 1591, 1583, 1541 (with a shoulder around 1560 cm^{-1}), 1483,

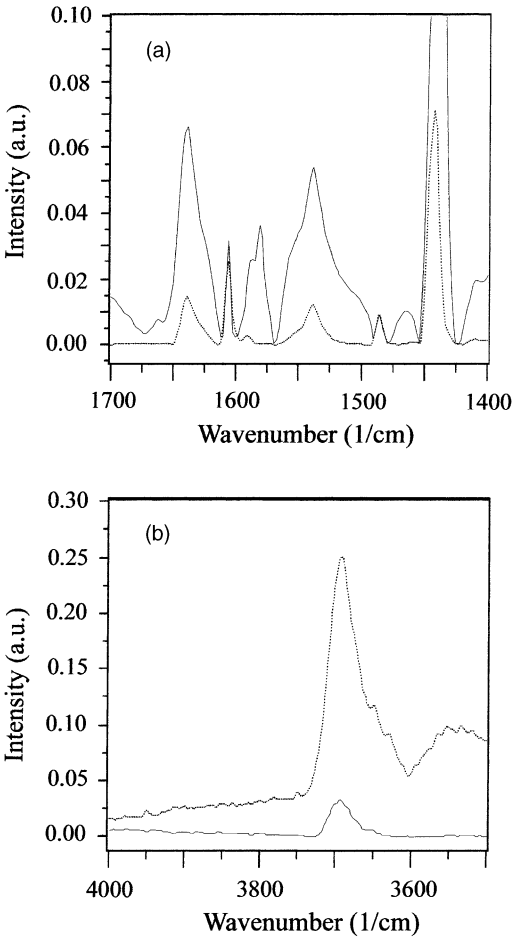

Fig. 3. IR spectra obtained after the exposure of the α-Fe_2O_3 (hematite) powder to the pyridine + N_2 mixture at RT (—), and after flowing N_2 for 10 min at RT (···).

1465 and 1443 cm^{-1}. The signal around 1583 cm^{-1} is consistent with the presence of a liquid layer of pyridine (which also contributes to the peak around 1443 cm^{-1}) [42]. Liquid-like pyridine can be easily removed by nitrogen and in fact the IR signals observed after the N_2 treatment are centred around 1639, 1606, 1591, 1574 (weak), 1541, 1483 and 1443 cm^{-1} (Table 3 and Fig. 3a). The position of these peaks indicates the presence of pyridine bonded to B_s^a (hereafter py-B_s^a, 1639 and 1541 cm^{-1}) and L_s^a (hereafter py-L_s^a 1606, 1483 and 1443 cm^{-1}) [22,43]. Moreover, the feature at 1591 cm^{-1} agrees with the formation of pyridine H-bonded to the Fe_2O_3 surface [4].

Table 3
FTIR data (cm^{-1}) of pyridine adsorbed on hematite; the reference data concerning pyridine are also reported

	Py/Fe_2O_3 (this work)	Pyridine[a]
8a	1639 1606	1583 (vs.)
8b	1591 1574 1541	1572 (m)
19a	1483	1482 (s)
19b	1443	1441 (vs.)

[a] [63].

As far as the strength of the L_s^a is concerned, the quite low shift of the peak 8a (see Fig. 3) upon chemisorption (from 1583 to 1606 cm^{-1}: $\Delta\nu$ = 23 cm^{-1}) suggests the presence of medium strength L_s^a [22,44].

Moving to the region of the O–H stretchings (Fig. 3b) the peak at 3700 cm^{-1} suggests the presence of free OH groups. Furthermore, its intensity increases after exposure to N_2 and the further peak appearing at ca. 3550 cm^{-1} is in theme with the formation of H-bonded OH groups. As a whole, these data seem to suggest that pyridine interacts with the OH groups distributed on the α-Fe_2O_3 surface [4,42] and that the N_2 flow has the capability to remove the weakly chemisorbed species.

In a previous paper [19] we suggested that water molecules H-bonded to the isolated hydroxyl groups have the effect of shifting their O–H stretching from 3720 to 3620–3630 cm^{-1}. Water can be removed by heating treatments (as confirmed by the intensity increment of the peak at ca. 3720 cm^{-1}).

In the present case no heating treatment has been carried out before exposure, thus we can assume the OH groups at 3622 cm^{-1} bonded to the water molecules. Pyridine molecules can interact with the free (3740 and 3690–3700 cm^{-1}) or H-bonded OH groups (3663 cm^{-1}). The interaction with the H-bonded hydroxyl groups can free new OH groups justifying the increase of the peak at 3700 cm^{-1} observed after the exposure to pyridine. Moreover, the intensity increase of the isolated and H-bonded OH groups follows from the pyridine desorption.

The IR spectrum of the α-Fe_2O_3 exposed to pyridine at RT and heated at 373 K for 10 min is reported

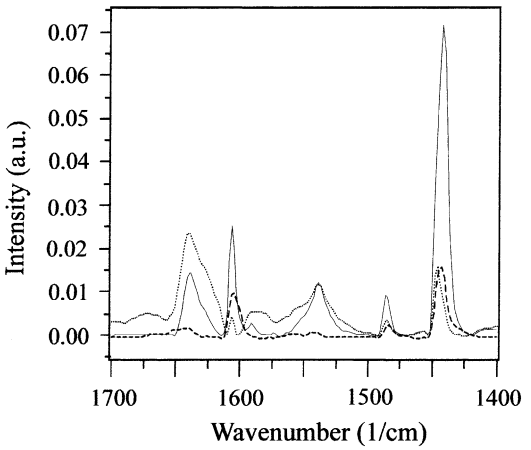

Fig. 4. IR spectra obtained after the exposure of the α-Fe_2O_3 (hematite) powder to the pyridine+N_2 mixture at RT (—), and after heating the obtained system at 373 K (···); IR spectra obtained after the exposure of the α-Fe_2O_3 (hematite) powder to the pyridine+N_2 mixture at 473 K (- - -).

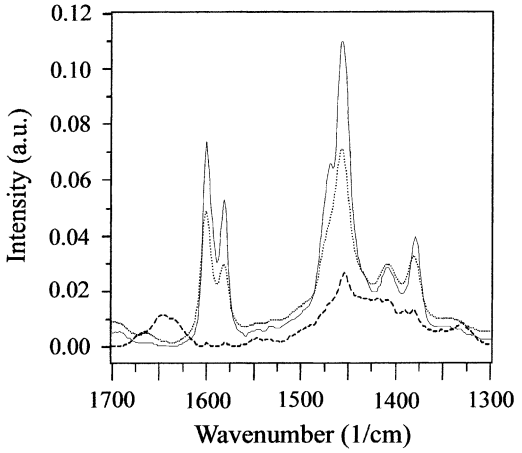

Fig. 5. IR spectra obtained after the exposure of the α-Fe_2O_3 (hematite) powder to the 2,6-dimethyl pyridine (lutidine) + N_2 mixture at RT (—), after exposure of the obtained system to a N_2 flow for 10 min at RT (···) and after heating treatment to 373 K (- - -).

in Fig. 4. The intensity of the py-L_s^a peaks decreases more than that of the py-B_s^a, thus suggesting that the bond between pyridine and the L_s^a is weaker than the bond between pyridine and the B_s^a.

The spectra obtained after exposure of the α-Fe_2O_3 powder to pyridine at 373 K are shown in Fig. 4. As it can be observed the py-L_s^a/B_s^a peaks intensity ratio increases with the temperature of exposure (from 1.7 at RT to 4.7 at 373 K) suggesting that the treatment at 373 K causes the decrease of the B_s^a, probably because of the condensation of adjacent OH groups.

This result is consistent with the behaviour observed for the α-Fe_2O_3 powder heated at increasing temperatures. As a mater of fact the heating treatment of the hematite powder causes the intensity decrease of the peaks attributed to the H-bonded hydroxyl groups centred around 3663 and 3622 cm^{-1} (Fig. 2).

The chemisorption of pyridine was also carried out under HV conditions and followed by means of XPS and QMS. Both the Fe 2p and O 1s peaks position and shape and the O/Fe atomic ratio do not change after exposure to pyridine at RT or at higher temperatures. These results suggest that the interaction with pyridine does not induce any alteration of the α-Fe_2O_3 surface. Moreover, the QMS results never show, at temperature lower than 473 K, the presence of species derived from the oxidation or decomposition of pyridine.

It is of relevance to note that the presence of pyridine on the iron oxide surface was never revealed by XPS (at exposure temperatures between RT and 473 K) [45][2] . This may indicate that the interaction between pyridine and hematite surface is not strong enough to withstand the vacuum conditions. Incidentally, it is worth of note that the vacuum conditions also cause the condensation of the weakly bonded OH groups and the decrease of the Brönsted acidity.

3.3. Reaction with 2,6-dimethyl pyridine

The IR spectrum of the α-Fe_2O_3 obtained after exposure at RT to a lutidine + N_2 mixture is shown in Fig. 5. The spectrum investigation reveals the presence of several peaks centred around 1602, 1583, 1470 and 1458 cm^{-1}. Lutidine is a probe molecule more specific than pyridine with respect to the B_s^a when adsorption is perpendicular to the planar surfaces. This characteristic relies on the steric hindrance of the probe molecule as well as on its higher basicity ($pK_a = 6.7$ for lutidine and 5.2 for pyridine) [26]. Once again, the IR peaks observed after exposure to the lutidine

[2] Incidentally, the sensitivity of XPS range around the atomic percent that is usally enough to allow the observation of less than a monolayer grown on a surface at this purpose.

Table 4
FTIR data (cm^{-1}) of 2,6-dimethyl pyridine (lutidine) adsorbed on hematite; the reference data concerning 2,6-dimethyl pyridine are also reported

	L/Fe_2O_3	Lutidine[a]
8a	1645 1603	1590
8b	1580	1582
19a		1470
19b	1455–1457	1460

[a] [64].

are compatible with the presence of a liquid layer of lutidine and analogously to the pyridine case, IR spectrum obtained after the N_2 treatment (Fig. 5), clearly shows that liquid-like lutidine is easily removed.

IR peaks observed after the N_2 exposure, (Table 4 and Fig. 5), are centred around 1603, 1580 and 1455–1457 cm^{-1} and suggest the presence of 2,6-dimethyl pyridine co-ordinated to the surface acid sites.

The IR spectrum of the α-Fe_2O_3 exposed to lutidine at RT and heated at 373 K (for 10 min) is shown in Fig. 5. The inspection of the spectrum shows the presence of the 2,6-dimethyl pyridinium ion as indicated by the two peaks centred around 1645 and 1455–1457 cm^{-1} [46]. The existence of the pyridinium ions confirms the presence of exposed B_s^a.

In contrast to that, the heating treatment causes the condensation of the OH groups and then the abrupt decrease of the Brönsted acid sites as confirmed by the IR spectrum obtained after the exposure of the Fe_2O_3 powder at the 2,6-dimethyl pyridine at 473 K: as a matter of fact, no traces of lutidine bonded to the oxide surface are evident at this temperature.

3.4. Reaction with carbon monoxide and carbon dioxide

The interaction between CO and α-Fe_2O_3 is still a controversial matter and several authors obtained different results [47–50].

The IR spectrum recorded after the chemisorption of the CO at ca. 143 K is shown in Fig. 6. The spectrum investigation reveals the presence of a broad peak centred around 2020–2060 cm^{-1}; the peak position testifies a red-shift phenomena. It is noteworthy that our results are not inconsistent with the terminal carbonyls

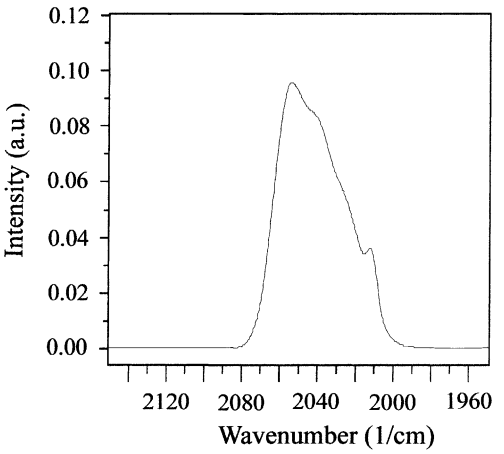

Fig. 6. IR spectrum obtained after the exposure of the α-Fe_2O_3 (hematite) powder to the CO at 143 K.

frequencies observed for the iron (III) carbonyl complexes (50 $cm^{-1} < \Delta\nu < 100\ cm^{-1}$) [51]. Moreover, a similar behaviour was observed by Casarin et al. for the interaction of CO with Ti_2O_3 [52].

The broad band shape suggests the presence of several contributions, and thus of non equivalent Lewis acid sites on the Fe_2O_3 surface. The fitting procedure allows to individuate four contributions centred around 2054, 2041, 2024 and 2012 cm^{-1} corresponding to the existence of different acid sites.

The shift values (with respect to the C–O stretching value of the free CO molecule) agree with the presence of middle and high acid strength sites. In the case of the iron oxide the experimental CO stretching frequency is a complex function of the Lewis acidity of the cations and of its π-electron donating power; [22] still the heterogeneity of the acid sites distribution on the hematite surface can be suggested by the experimental outcomes.

Several Author attempted to compare the behaviour of polycrystalline samples and well-defined model surfaces. This correspondence is not so straightforward for hematite. α-Fe_2O_3 natural growth faces are the (0 0 1) and (0 1 2) [53]. As a matter of fact the reactivities of the α-Fe_2O_3 (0 0 1) surface and of a powder sample are different: as an example, methanol adsorbs molecularly on the α-Fe_2O_3 (0 0 1) surface [54] while the interaction is mainly dissociative on the nanopowders [18]. Moreover, IR results suggest a mechanism

of esterification involving the OH groups distributed on the oxide surface [18][3] .

In powder samples the predominantly exposed faces depend on the preparation procedure and particle size; [55] α-Fe_2O_3 microcrystals exposing preferentially low index faces (mainly prismatic) can be obtained by thermal decomposition of α-FeO(OH) [48].

In our nanocrystalline sample both prismatic and hexagonal dipyramidals faces seem to be evident (Table 1). In high oxygen pressure condition spin-density functional theory ab initio calculation predicted an unrecostructed and relaxed α-Fe_2O_3 (0 0 1) surface oxygen terminated [56]. Five-fold coordinated iron ions and threefold coordinated oxygen atoms are present on the (0 1 2) and (1 1 0) faces while higher coordinative unsaturation is expected for Fe^{3+} ions exposed on the (1 1 3) surface. This heterogeneous situation can give reason of the IR data.

Moreover, the surface hydroxylation needs to be considered because of its effect on the surface structure.

The Fe terminated (0 0 1) surface, as an example, should be characterized by a top layer of three-fold coordinated iron ions in hexagonal arrangement. Molecular dynamics calculations on the hydroxylated surface suggest that the relaxation energy tends to keep the iron layer in a four-fold coordinated state [57].

Moreover, in powder samples structural and chemical defects can play an important role in surface reactivity: low coordinated Fe^{3+} ions, as an example, can be exposed in edge and corners.

The IR peak observed after exposure to CO (2054, 2041, 2024 and 2012 cm^{-1}) can be tentatively assigned to the interaction with five-, tetra- and three-fold coordinated Fe^{3+} ions but further experimental and theoretical investigations are needed.

[3] On an "ideal" dehydroxylated surface, the mechanism can be dissociative, to produce hydroxyl and alkoxy groups, or molecular, by interaction of the alcohol molecules with Lewis acid or basic sites. Other chemisorption modes can be possible on an hydroxylated surface: replacement of molecular water present on the surface; esterification with acid surface hydroxyls reversible adsorption on the surface hydroxyls. Methanol is chemisorbed mainly dissociatively whereas molecular chemisorption is prevalent in higher alcohols. When methanol is chemisorbed, Heating treatment at $T > 400$ K induces the formation of formate while hydrocarbons are the main products of the other alcohols.

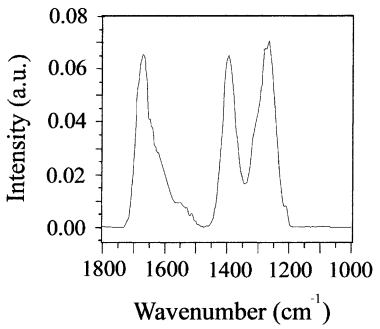

Fig. 7. IR spectrum obtained after the exposure of the α-Fe_2O_3 (hematite) powder to the CO_2 at RT: region between 1000 and 1800 cm^{-1}.

The IR spectrum obtained after exposing the α-Fe_2O_3 to CO_2 at RT is shown in Fig. 7. The spectral region between 1200 and 1750 cm^{-1} includes several peaks at ca. 1671 (with shoulders around 1650 and 1620 cm^{-1}), 1556, 1396 and 1269 cm^{-1} (with a shoulder around 1316 cm^{-1}). The position of the bands at 1671, 1396 and 1269 (Table 5) is indicative of the formation of surface bicarbonate species [58,59] as a consequence of the interaction between CO_2 and the surface OH. At variance to that the weak contributions around 1556 and 1316 cm^{-1} agree with the formation of surface bidentate carbonate species [58–61] as a consequence of the adsorption of CO_2 on a Lewis acid/base site constituted by the metal ion and the neighbouring oxide ion [62].

Rochester et al. [4] studied the interaction between CO_2 and an α-Fe_2O_3 (hematite) powder synthesised by decomposition of a ferrigel precipitate (obtained by mixing aqueous solution of NaOH and $FeCl_3$). These authors observed a peak centred around 1320 cm^{-1} after the exposure at CO_2 of an hematite powder heated at 713 K while no evidence for the adsorption of CO_2 could be detected on hematite heated at 973 K.

In our case, the presence of the bicarbonate species is well evident and suggests a high hydroxylation of the surface; the surface bidentate carbonate species form in a lesser extent.

The chemisorption of carbon dioxide was also carried out under HV conditions and followed by means of XPS and QMS. The Fe 2p and O 1s XPS peaks position and shape as well as the surface atomic composition, do not change after the exposure to CO_2 at

Table 5
FTIR data (cm^{-1}) of carbon dioxide adsorbed on Fe_2O_3 powder; the reference data concerning carbonate and bicarbonate species are also reported[a]

	CO_2/Fe_2O_3 (this work)	Carbonate	Complex	Organic	Bicarbonate
C=O stretching			1577–1493	1870–1750	1630–1620
Asymmetrical stretching C–O	1671	1420–1470	1338–1260	1280–1252	1410–1400; 1370–1290
Symmetrical stretching C–O	1396		1082–1055; 1050–1021	1021–969	1050–1010; 1000–990
O–H bending	1269				

[a] [58].

RT or at higher temperatures (Fig. 1). This result suggest that the interaction between α-Fe_2O_3 and CO_2 is weak and cannot withstand the vacuum conditions. Moreover, the QMS results never show, at temperature lower than 473 K, species derived from the decomposition of the carbon dioxide.

4. Conclusions

In this paper the interaction between α-Fe_2O_3 and pyridine, lutidine, CO and CO_2 was studied.

The α-Fe_2O_3 powder was prepared by precipitation from and acid solution of iron (III) ions. The oxide has the crystallographic structure of hematite and it is characterised by the presence of Fe–OH bonds; both isolated and H-bonded OH groups are present.

The reactivity of this powder with respect to pyridine, 2,6-dimethyl pyridine, carbon monoxide and carbon dioxide was investigated both at atmospheric pressure (by means of FTIR) and under HV conditions (by means of XPS and QMS).

1. As far as the interaction between pyridine and α-Fe_2O_3 is concerned our results indicate the presence, on the oxide surface, of both Lewis (L_s^a) and Brönsted (B_s^a) acid sites.
2. 2,6-Dimethyl pyridine (lutidine) interacts with the α-Fe_2O_3 indicating the presence of exposed B_s^a easy accessible to the sterically hindered 2,6-dimethyl pyridine.
3. The carbon monoxide chemisorption reveals the presence of several non-equivalent L_s^a; it has also to be observed that the formation of the L_s^a –CO complexes on the iron oxide surface red-shifts the IR C–O stretching frequency.
4. CO_2 interacts with the OH groups distributed on the Fe_2O_3 surface forming bicarbonate species. Moreover the IR data agree with the formation of surface bidentate carbonate suggesting the presence of active sites constituted by a metal ion and the neighboring oxygen.
5. The evacuation of the reaction chamber by means of nitrogen and thermal treatments at 373 and 473 K have been used to investigate the strength of the acid sites.
6. The chemisorption of pyridine and of CO_2 under HV conditions never reveals the presence of molecules interacting with the surface, thus confirming that the interaction between CO_2 and surface active sites is weak. It is noteworthy that the interaction never causes the modification of the α-Fe_2O_3 surface.
7. QMS results show that the probe molecules were never decomposed by the oxide surface confirming their validity as acid/base sites test molecules.

Acknowledgements

The authors thank Prof. E. Tondello and Prof. M. Casarin for helpful discussions and suggestions during this work; the authors also thank Prof. P. Colombo for the XRD spectra.

References

[1] C.K. Rofer-DePoorter, Chem. Rev. 81 (1981) 447.
[2] H.H. Kung, in: Transition Metal Oxides: Surface Chemistry and Catalysis, Elsevier, Amsterdam, 1989.
[3] J. Novakova, P. Jiru, V. Zavadil, J. Catal. 21 (1971) 143.
[4] C.H. Rochester, S.A. Topham, J. Chem. Soc., Faraday Trans. 75 (1979) 1259.
[5] G. Busca, N. Cotena, Mater. Chem. 3 (1978) 49.
[6] G. Busca, V. Lorenzelli, Mater. Chem. 5 (1980) 213.
[7] G. Busca, V. Lorenzelli, J. Catal. 66 (1980) 155.

[8] V. Lorenzelli, G. Busca, N. Sheppard, J. Catal. 66 (1980) 28.
[9] G. Busca, V. Lorenzelli, Mater. Chem. 6 (1981) 175.
[10] G. Busca, V. Lorenzelli, J. Catal. 72 (1981) 303.
[11] G. Busca, V. Lorenzelli, J. Chem. Soc., Faraday Trans. 178 (1982) 2911.
[12] G. Busca, React. Kinet. Catal. Lett. 20 (1982) 373.
[13] G. Busca, P.F. Rossi, Mater. Chem. Phys. 9 (1983) 561.
[14] G. Busca, T. Zerlia, V. Lorenzelli, A. Girelli, J. Catal. 88 (1984) 125, 131.
[15] G. Busca, T. Zerlia, V. Lorenzelli, A. Girelli, React. Kinet. Catal. Lett. 27 (1985) 429.
[16] T. Iizuka, H. Ikeda, T. Terao, K. Tanabe, Aust. J. Chem. 35 (1982) 927.
[17] T. Ishikawa, W.Y. Cai, K. Kandori, Langmuir 9 (1993) 1125.
[18] A. Glisenti, G. Favero, G. Granozzi, J. Chem. Soc., Faraday Trans. 94 (1998) 173.
[19] A. Glisenti, J. Chem. Soc., Faraday Trans. 94 (1998) 3671.
[20] V.E. Heinrich, P.A. Cox, The Surface Science of Metal Oxides, Cambridge University Press, Cambridge, 1994.
[21] A. Glisenti, J. Mol. Catal. A: Chem. 153 (2000) 169.
[22] G. Busca, Catal. Today 41 (1998) 191.
[23] H.A. Benesi, J. Catal. 28 (1973) 176.
[24] P.A. Jacobs, C.P. Heylen, J. Catal. 34 (1974) 267.
[25] E.R.A. Matulewicz, F.P.J.M. Kerkhof, J.A. Moulijn, H.J.J. Reitsma, Colloid Interf. Sci. 77 (1980) 110.
[26] A. Corma, C. Rodellas, V. Fornes, J. Catal. 88 (1984) 374.
[27] S.G. Lias, S.E. Stein, NIST/EPA/MSDC Mass Spectral Database, PC version 3.0, June 1990.
[28] E.I. Ko, J.B. Benzinger, R.J. Madix, J. Catal. 62 (1980) 264.
[29] P. Kubelka, F. Munk, Z. Techol. Phys. 12 (1931) 593.
[30] G. Kortum, Reflectance Spectroscopy, Springer, New York, 1969.
[31] D.A. Shirley, Phys. Rev. 55 (1972) 4709.
[32] J.F. Moulder, W.F. Stickle, P.E. Sobol, K.D. Bomben, in: J. Chastain (Ed.), Handbook of X-ray Photoelectron Spectroscopy, Physical Electronics, Eden Prairie, MN, 1992.
[33] Joint Committe on Powder Diffraction Standards: card number 33-664.
[34] S. Enzo, S. Polizzi, A. Benedetti, Z. Kristall, 170 (1985) 275.
[35] N.S. McIntyre, T.C. Chan, in: D. Briggs, M.P. Seah (Eds.), Practical Surface Analysis, Vol. 1, 2nd Edition, Wiley, New York, 1990 (Chapter 10).
[36] N.S. McIntyre, D.G. Zetaruk, Anal. Chem. 49 (1977) 1521.
[37] X-ray Photoelectron Spectroscopy Database 20, version 3.0, National Institute of Standards and Technology, Gaithersburg, MD.
[38] H.-P. Boehm, H. Knözinger, in: J.R. Anderson, M. Boudart (Eds.), Catalysis: Science and Technology, Vol. 4, Verlag, Berlin, 1983 (Chapter 2).
[39] Y. Suda, T. Morimoto, M. Nagao, Langmuir 3 (1987) 99.
[40] L.H. Little, in: Infrared Spectra of Adsorbed Species, Academic Press, San Diego, CA, 1966 (Chapter 3).
[41] C.H. Rochester, S.A. Topham, J. Chem. Soc., Faraday Trans. 1 (75) (1979) 591, 1073.
[42] C. Morterra, A. Chiorino, G. Ghiotti, E. Garrone, J. Chem. Soc., Faraday Trans. 1 75 (1979) 271.
[43] K. Tanabe, in: J.R. Anderson, M. Boudart (Eds.), Catalysis: Science and Technology, Vol. 2, Springer, Berlin, 1981 (Chapter 5).
[44] V. Lorenzelli, G. Busca, N. Sheppard, J. Catal. 66 (1980) 28.
[45] C.S. Fadley, S.A.L. Bergström, in: D.A. Shirley (Ed.), Electron Spectroscopy, North-Holland, Amsterdam, 1972.
[46] L. Cerrsin, B.J. Fax, R.C. Lord, J. Chem. Phys. 21 (1953) 1170.
[47] G. Blyholder, E.A. Richardson, J. Phys. Chem. 66 (1962) 2597.
[48] A. Zecchina, D. Scarano, A. Reller, J. Chem. Soc., Faraday Trans. 1 84 (1988) 2327.
[49] H. Batis, N. Harrouch, A. Ghorbel, J. Soc. Chim. Tunis. 2 (1985) 51.
[50] A. Zecchina, D. Scarano, S. Bordiga, G. Spoto, C. Lamberti, Adv. Catal. 46 (2001) 265.
[51] H.-F. Hsu, S.A. Kock, C.V. Popescu, E. Münck, J. Am. Chem. Soc. 119 (1997) 8371;
B.A. Etzenhouser, M. DiBiase Cavanaugh, H.N. Spurgeon, M. Sponsler, J. Am. Chem. Soc. 116 (1994) 2221;
M.-H. Delville-Desbois, S. Mross, D. Astruc, J. Linares, F. Varret, H. Rabaâ, A. Le Beuze, J.-Y. Saillard, R.D. Culp, D. Atwood, A.H. Cowley, J. Am. Chem. Soc. 118 (1996) 4133;
J. Morrow, D. Catheline, M.-H. Desbois, J.-M. Manriquez, J. Ruiz, D. Astruc, Organometallics 6 (1987) 2605;
M.J. Therien, W.C. Trogler, J. Am. Chem. Soc. 109 (1987) 5127.
[52] M. Casarin, C. Maccato, A. Vittadini, J. Phys. Chem. B. 106 (2002) 795.
[53] W.C. Mackrodt, R.J. Davey, S.N. Black, R. Docherty, J. Cryst. Growth 80 (1987) 441.
[54] Q. Guo, P.H. McBreen, P.J. Møller, Surf. Sci. 423 (1999) 19.
[55] V. Shklover, M.-K. Nazeeruddin, S.M. Zakeeruddin, C. Barbé, A. Kay, T. Haibach, W. Steurer, R. Hermann, H.-U. Nissen, M. Grätzel, Chem. Mater. 9 (1997) 430.
[56] X.-G. Wang, W. Weiss, Sh.K. Shaikhutdinov, M. Ritter, M. Petersen, F. Wagner, R. Schlögl, M. Scheffler, Phys. Rev. Lett. 81 (1998) 1038.
[57] E. Wasserman, J.R. Rustad, A.R. Felmy, B.P. Hay, J.W. Halley, Surf. Sci. 385 (1997) 217.
[58] B.M. Gatehouse, S.E. Livingstone, R.S. Nyholm, J. Chem. Soc. (1958) 3137.
[59] L.H. Little, Infrared Spectra of Adsorbed Species, Academic Press, San Diego, CA, 1966 (Chapter 3).
[60] C. Morterra, A. Zecchina, S. Coluccia, A. Chiorino, J. Chem. Soc., Faraday Trans. 1 73 (1977) 1544.
[61] C. Morterra, G. Cerrato, V. Bolis, B. Fubini, Spectrochim. Acta 49A (1993) 1269.
[62] A. Auroux, A. Gervasini, J. Phys. Chem. 94 (1990) 6371.
[63] L. Corrsin, B.J. Fax, R.C. Lord, J. Chem. Phys. 21 (1953) 1170.
[64] R.L. Bohon, R. Isaac, H. Hoftiezer, R.J. Zellner, Anal. Chem. 30 (1958) 245.